Quantifying the impact of model errors on top-down estimates of carbon monoxide emissions using satellite observations

Zhe Jiang,[1] Dylan B. A. Jones,[1] Monika Kopacz,[2] Jane Liu,[3] Daven K. Henze,[4] and Colette Heald[5]

Received 4 November 2010; revised 7 April 2011; accepted 10 May 2011; published 11 August 2011.

[1] We conduct inverse analyses of atmospheric CO, using the GEOS-Chem model and observations from the Measurement of Pollution in the Troposphere satellite instrument, to quantify the potential contribution of systematic model errors on top-down source estimates of CO. We assess how the specification of the source of CO from the oxidation of biogenic nonmethane volatile organic compounds (NMVOCs) in the inversion impacts the top-down estimates. Our results show that when the NMVOC source of CO is comparable to or larger than the combustion source, optimizing the CO from NMVOC emissions on larger spatial scales than the combustion emissions could result in significant overadjustment for the a posteriori CO emissions and could lead to negative sources of CO, such as we found for the top-down South American emissions in June. We quantify the impact of aggregation errors on the source estimates, associated with conducting the inversion at a lower resolution than the atmospheric model. We find that aggregating the emissions across spatial scales in which the a priori error in the emissions changes sign could introduce biases exceeding 20% in the flux estimates since the inversion cannot correct the a priori error by uniformly scaling the emissions across the region. We also use the GEOS-3 and GEOS-4 meteorological fields in GEOS-Chem to examine the impact of discrepancies in atmospheric transport and in the atmospheric OH distribution on the source estimates. We find that the differences in the OH distribution and transport fields associated with the GEOS-3 and GEOS-4 products introduce comparably large differences of as much as 20% in the source estimates. Our results indicate that mitigating systematic model error is critical for improving the accuracy of the inferred source estimates.

Citation: Jiang, Z., D. B. A. Jones, M. Kopacz, J. Liu, D. K. Henze, and C. Heald (2011), Quantifying the impact of model errors on top-down estimates of carbon monoxide emissions using satellite observations, *J. Geophys. Res.*, *116*, D15306, doi:10.1029/2010JD015282.

1. Introduction

[2] Inverse modeling is a powerful tool for combining observations of atmospheric composition with models to improve our understanding of the atmosphere. In the past decade there has been an increasing use of inverse modeling to better quantify regional surface emissions of carbon monoxide (CO), which are uncertain. The recent inversion analysis by *Kopacz et al.* [2010], for example, found that the annual source of CO from East Asia, inferred from satellite observations, was about 65% larger than their a priori inventory. They found that the disagreement was seasonally dependent, with emissions in winter underestimated by more than a factor of two. Atmospheric CO is a product of incomplete combustion and a byproduct of the oxidation of hydrocarbons in the atmosphere. It plays a critical role in determining the oxidative capacity of the atmosphere, as it is the primary sink of OH. Its lifetime varies from a few weeks to a few months, which is sufficiently long to track pollution plumes on synoptic and intercontinental scales but short enough to provide strong pollution enhancements relative to background abundances. This makes CO an ideal tracer for inverse modeling.

[3] A major challenge with inverse modeling of atmospheric CO is that the "top-down" emissions inferred in the inversions typically depend on the inversion framework employed and the data sets exploited. This has resulted in significant differences in reported top-down emission estimates. Using the same satellite observations, *Stavrakou and Müller* [2006] reported an estimate of south Asian emissions of the 2000–2001 period that were 75% lower than those inferred by *Arellano et al.* [2004]. *Heald et al.* [2004] obtained

[1]Department of Physics, University of Toronto, Toronto, Ontario, Canada.
[2]Woodrow Wilson School of Public and International Affairs, Princeton University, Princeton, New Jersey, USA.
[3]Air Quality Research Division, Science and Technology Branch, Environment Canada, Downsview, Ontario, Canada.
[4]Department of Mechanical Engineering, University of Colorado, Boulder, Colorado, USA.
[5]Department of Atmospheric Science, Colorado State University, Fort Collins, Colorado, USA.

Copyright 2011 by the American Geophysical Union.
0148-0227/11/2010JD015282

an estimate of 192 Tg yr^{-1} for the total source of CO from China, Japan, and Korea using satellite observations, whereas they inferred a source of 142 Tg yr^{-1} based on aircraft observations, due to the different spatiotemporal coverage of the data sets. Using simple inversion approaches, *Allen et al.* [2004] and *Carmichael et al.* [2003] inferred a total Asian source of CO of 328 Tg yr^{-1} and 447 Tg yr^{-1}, respectively, compared to the 361 Tg yr^{-1} estimated by *Heald et al.* [2004] for the same period.

[4] Inversion analyses of atmospheric CO are also sensitive to systematic errors in the atmospheric models. *Kopacz et al.* [2009] found that when they conducted their inversion analysis at the resolution of the atmospheric model, to minimize biases associated with aggregating the CO sources to larger spatial scales, they obtained only a modest change in the emissions from Japan and Korea (11% for Japan and 6% for Korea), whereas their low-resolution inversion suggested a 69% increase in the Japanese and Korean emissions. *Stavrakou and Müller* [2006] found that the difference in their a posteriori emissions obtained with high- and low-resolution inversions could be larger than 20%. The discrepancies in the literature between the different top-down estimates of the regional CO sources suggest the need for a more comprehensive assessment of the uncertainty in the source estimates associated with these systematic errors.

[5] In this paper, we examine the potential impact of four different types of systematic model errors on the inferred CO sources. Using observations from the Measurement of Pollution in the Troposphere (MOPITT) satellite instrument, we focus on quantifying the CO sources in the tropics, where biogenic emissions and biomass burning provide strong, distinct sources of CO. We first examine the impact on the top-down estimates of how the source of CO from the oxidation of biogenic nonmethane volatile organic compounds (NMVOCs) is specified in the inversion analysis. In most studies [e.g., *Palmer et al.*, 2003; *Heald et al.*, 2004; *Arellano and Hess*, 2006; *Jones et al.*, 2009; *Kopacz et al.*, 2009] the biogenic NMVOC source is aggregated into a background global chemical source of CO. In contrast, *Stavrakou and Müller* [2006] explicitly solved for the biogenic NMVOC source at the same spatial resolution at which the combustion CO emissions (from fuel combustion and biomass burning) are constrained. We show that aggregating the biogenic NMVOC source into global background could result in significant overadjustment for the a posteriori CO emissions.

[6] The second source of model bias that we examine is aggregation error [*Kaminski et al.*, 2001], which can occur when the CO emissions are aggregated to a resolution that is coarser than the resolution of the forward model. Following the approach of *Stavrakou and Müller* [2006] and *Kopacz et al.* [2009], we conduct low- and high-resolution inversions to assess the impact of this error. The low-resolution inversion quantifies the sources on continental scales and is based on the Bayesian analytical inversion configuration of *Heald et al.* [2004], whereas the high-resolution analysis solves for the sources at the grid box scale and uses the approach of *Kopacz et al.* [2009]. We focus here on quantifying the bias in the source estimates, globally, associated with aggregating the CO fluxes across individual continental regions.

[7] We then assess the impact of errors in linearizing the CO chemistry in the inversion. To minimize the computation cost of the inversion, most inversion analyses of CO linearize the forward model using specified OH abundances to account for the chemical loss of CO [e.g., *Pétron et al.*, 2002; *Palmer et al.*, 2003; *Arellano et al.*, 2004; *Kopacz et al.*, 2009]. Although the lifetime of OH is short, its distribution reflects the influence of both chemistry and transport, with transport controlling the distribution of longer-lived OH precursors. Therefore, using an imposed OH distribution that is inconsistent with the transport field employed in the forward model introduces a linearization error in the simulated CO abundances. We examine here the impact of this linearization error on the inferred CO sources in our inversion analysis. We also investigate the effect of transport errors on the inversion analysis. In this context, we employ two different versions of the meteorological fields, GEOS-3 and GEOS-4, which drive the GEOS-Chem model. The key difference between these two sets of meteorological fields is that they have different convection schemes. We show that discrepancies in the transport and OH fields can have comparably large impacts in the top-down source estimates.

[8] In section 2 we begin with a brief description of the MOPITT instrument and the GEOS-Chem model. The inversion methodologies are presented in section 3, whereas the inversion results and error analysis is provided in section 4. In section 5 we provide a summary of the results and a discussion of their implications for future inversion analysis.

2. Observation Instrument and Model

2.1. MOPITT

[9] The MOPITT instrument is on board of the Terra satellite, which was launched on 18 December 1999, on NASA's Terra spacecraft in a Sun-synchronous polar orbit at an altitude of 705 km, with a 10:30 local time equator crossing. CO columns and profiles are retrieved from infrared (IR) emissions in the 4.7 μm region of the spectrum with a spatial resolution of 22 × 22 km^2. Its observing strategy consists of a 612 km cross-track scan and achieves complete global coverage every 3 days. The MOPITT retrievals are performed with an optimal estimation method [*Deeter et al.*, 2003]. We use version 3 MOPITT data, in which the retrieved mixing ratios are reported on 7 pressure levels in the troposphere (surface, 850, 700, 500, 350, 250 and 150 hPa). The retrieved CO profiles can be expressed as a linear estimate of the true atmospheric state:

$$\hat{\mathbf{z}} = \mathbf{z_a} + \mathbf{A}(\mathbf{z} - \mathbf{z_a}) + \mathbf{G}\varepsilon, \quad (1)$$

where $\mathbf{z_a}$ is the MOPITT a priori CO profile, $\mathbf{z}$ is the true atmospheric state, $\mathbf{A}$ is the MOPITT averaging kernel matrix and $\mathbf{G}\varepsilon$ describes the retrieval error. The MOPITT data have been extensively validated using aircraft and in situ measurements [*Emmons et al.*, 2004]. We filter the data following the recommended quality control criterion of neglecting retrievals with CO mixing ratios lower than 40 ppb [*Arellano et al.*, 2004].

[10] We use MOPPIT data for June and September 2000 and conduct one month inversions for these two months to assess how the impact of the model errors on the inversion is

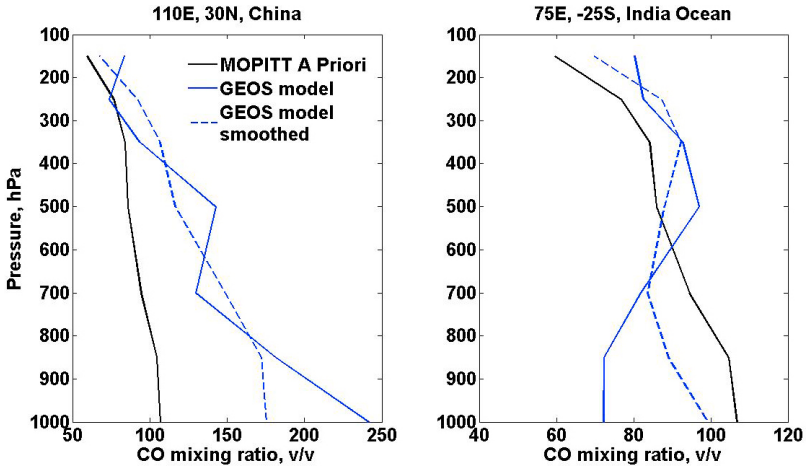

Figure 1. Influence of MOPITT retrieval on the vertical distribution of the modeled CO profile. The solid blue line is the raw modeled profile, the solid black line is the MOPITT a priori profile, and the dashed line is the transformed modeled profile, obtained using equation (2).

influenced by the strength of the sources. We selected June because it is before the biomass burning season in South America and when biomass burning in South Africa is weak. During September, on the other hand, biomass burning emissions from South America and South Africa are strong. Also, since our focus is on the tropics, we use MOPITT data only between 40°S and 40°N, and consider only daytime data since the nighttime retrievals have lower sensitivity to CO [*Deeter et al.*, 2007a].

[11] Because of the low sensitivity of MOPITT to CO in the lower troposphere over the oceans (as a result of the low surface-atmosphere thermal contrast) and over the tropical rain forests in South America and Africa [*Deeter et al.*, 2007a], we use only upper tropospheric CO columns, based on retrievals at 500, 350, 250 and 150 hPa. The influence of this low sensitivity is illustrated in Figure 1, where we show the smoothing influence of the MOPITT retrieval on modeled CO profiles over China and the Indian Ocean. The modeled profiles were transformed with the MOPITT a priori profile and averaging kernels using the expression

$$\hat{\mathbf{z}}^{\mathbf{mod}} = \mathbf{z_a} + \mathbf{A}\left(\mathbf{z}^{\mathbf{mod}} - \mathbf{z_a}\right), \tag{2}$$

which is analogous to equation (1). Here $\mathbf{z}^{\mathbf{mod}}$ is the GEOS-Chem profile and $\hat{\mathbf{z}}^{\mathbf{mod}}$ is the transformed profile, which captures the smoothing influence of the averaging kernels and the a priori bias. Over China, the transformed profile captures well the model profile down to about 800 hPa. Over the Indian Ocean, however, the transformed profile captures the profile down to about 600 hPa. Furthermore, *Deeter et al.* [2007b] showed that version 3 MOPITT retrievals can overestimate CO in the lower troposphere under low-CO conditions, such as in the southern hemisphere, compared to the version 4 retrievals. In their inversion analysis of the version 3 MOPITT data, *Jones et al.* [2009] used retrievals between 700 and 250 hPa, and *Arellano et al.* [2004] showed that using different vertical levels of the MOPITT retrievals produces differences in the inferred source estimates. There is clearly the need to better assess how the vertical distribution of information in the MOPITT retrievals influences the top-down estimates. However, the focus of our analysis here is on the model biases.

2.2. GEOS-Chem Forward Model

[12] The GEOS-Chem model (http://www.geos-chem.org) is a global 3-D chemical transport model (CTM) driven by assimilated meteorological observation from the NASA Goddard Earth Observing System (GEOS) at the Global Modeling and Data Assimilation Office. We use versions v6-02-05 and v7-02-04 of GEOS-Chem, at a horizontal resolution of 2° × 2.5°. We use v7-02-04 for the low-resolution inversion and exploit the adjoint of v6-02-05 for the high-resolution inversion. Version v7-02-04 of GEOS-Chem has an updated treatment of aerosols, but because our analysis is based on the CO-only simulation in GEOS-Chem, which uses archived monthly OH fields from the full chemistry runs, the differences between these versions of the model are inconsequential for our analyses. The OH fields used in our GEOS-3 simulations are from *Evans and Jacob* [2005], whereas for the GEOS-4 simulations we use OH fields archived from a full chemistry run of v7-02-04. The differences in these archived OH fields are discussed in section 4.3.

[13] The a priori fossil fuel CO emission in this work is from *Bey et al.* [2001]. It consists of a base emission inventory for 1985, which is scaled for 1998, as described by *Bey et al.* [2001] and *Duncan et al.* [2007]. The a priori biofuel (which includes woodfuel and agricultural waste) and biomass burning sources are based on the works by *Yevich and Logan* [2003] and *Duncan et al.* [2003], respectively. The chemical source of CO from the oxidation of methane (CH_4) and NMVOCs is treated following *Duncan et al.* [2007], in which the CO is emitted directly into the atmosphere assuming instantaneous oxidation of the NMVOC precursor, with specified yields of CO per atom of carbon oxidized. As noted by *Duncan et al.* [2007], this treatment may overestimate the CO source from long-lived NMVOCs, but is acceptable for short-lived NMVOCs such as isoprene and monoterpenes, which are the dominant biogenic NMVOCs. The oxidation of coemitted nonbiogenic

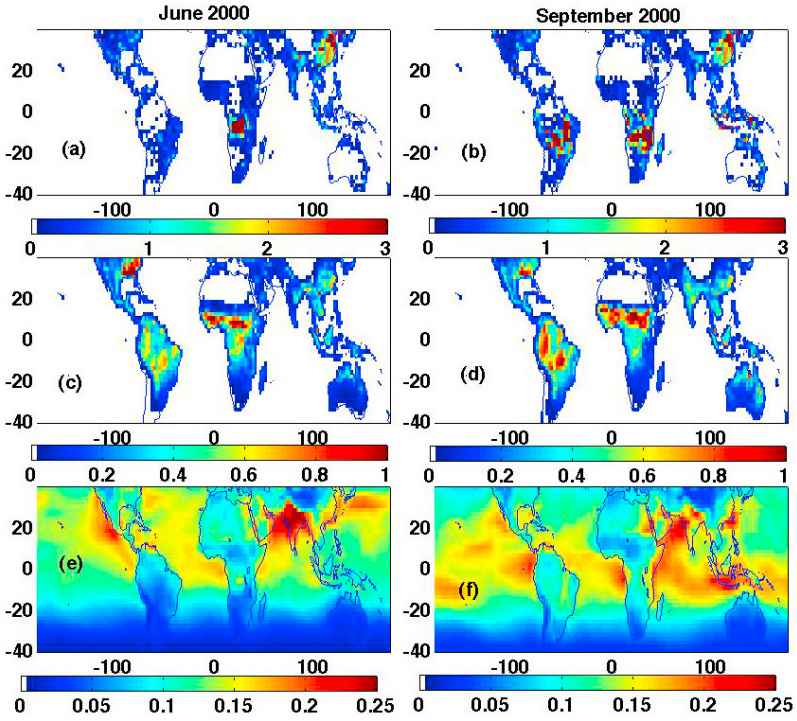

Figure 2. Distribution of the a priori CO sources in GEOS-Chem. (a, b) Combustion emissions from fossil fuel, biofuel, and biomass burning. (c, d) CO sources from biogenic NMVOCs. (e, f) CO from methane oxidation. Units are 10^8 kg/month (note the scales are different).

NMVOCs from combustion is modeled by increasing primary CO emissions by 19% and 11% for emissions from fuel combustion and biomass burning, respectively [*Duncan et al.*, 2007]. Figure 2 shows the a priori CO source from combustion (from fossil fuel, biofuel, and biomass burning) and from the oxidation of methane and biogenic NMVOCs. The annual global sources are 1127 Tg CO from fossil fuel, biofuel and biomass burning, 481 Tg CO from the oxidation of biogenic NMVOCs, and 840 Tg CO from the oxidation of CH_4.

[14] Two different versions of the GEOS meteorological fields are used in this work, GEOS-3 and GEOS-4. A key difference between these is in the convection schemes used in the GEOS general circulation model. GEOS-3 used the Relaxed Arakawa-Schubert (RAS) scheme [*Arakawa and Schubert*, 1974], whereas GEOS-4 used the Zhang and McFarlane (ZM) scheme [*Zhang and McFarlane*, 1995] for deep convection and the *Hack* [1994] scheme for shallow convection. Both models extend from the surface to 0.01 hPa, but the GEOS-3 fields have about 10 levels in the boundary layer, whereas GEOS-4 has only about 5 levels in the boundary layer. *Folkins et al.* [2006] compared the convection parameterizations in the two models and found that the convective outflow in the upper troposphere is weaker with the RAS scheme in GEOS-3 than with the ZM scheme in GEOS-4.

3. Inversion Methodology

[15] The inverse method seeks an optimal estimate of the CO sources consistent with both the observed atmospheric concentrations and the a priori constraints on the sources. In this inverse problem, the state vector of emissions, $\mathbf{x}$, and the observed concentrations, $\mathbf{y}$, are connected by a forward model $\mathbf{F}(\mathbf{x})$:

$$\mathbf{y} = \mathbf{F}(\mathbf{x}) + \varepsilon, \tag{3}$$

where ε is the observation error which includes contributions from the measurements and imperfections in the forward model. Assuming that the distribution of the errors is Gaussian, the objective of the inverse problem is equivalent to minimizing the cost function $J(\mathbf{x})$ [*Rodgers*, 2000]:

$$J(\mathbf{x}) = (\mathbf{F}(\mathbf{x}) - \mathbf{y})^{\mathbf{T}}\mathbf{S}_{\Sigma}^{-1}(\mathbf{F}(\mathbf{x}) - \mathbf{y}) + (\mathbf{x} - \mathbf{x_a})^{\mathbf{T}}\mathbf{S}_{\mathbf{a}}^{-1}(\mathbf{x} - \mathbf{x_a}). \tag{4}$$

Here $\mathbf{x_a}$ is the a priori estimate and $\mathbf{S}_{\Sigma}$ and $\mathbf{S_a}$ are the observational and a priori error covariance matrices, respectively. The first term on the right in equation (4) represents the mismatch between the simulated and observed concentrations weighted by the error covariance of the system. The second term represents the departure of the estimate from the a priori.

[16] To minimize the cost function, we solve

$$\nabla_{\mathbf{x}} J(\mathbf{x}) = 2\nabla_{\mathbf{x}}\mathbf{F}^{\mathbf{T}}\mathbf{S}_{\Sigma}^{-1}(\mathbf{F}(\mathbf{x}) - \mathbf{y}) + 2\mathbf{S}_{\mathbf{a}}^{-1}(\mathbf{x} - \mathbf{x_a}) = 0, \tag{5}$$

where $\nabla_{\mathbf{x}}\mathbf{F}$ is the Jacobian matrix of the forward model, which gives the sensitivity of the CO abundances to emissions. The maximum a posteriori (MAP) estimate for the

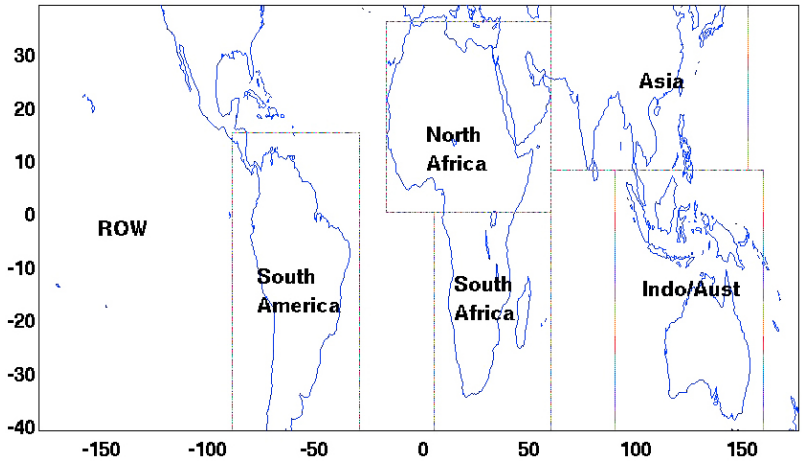

Figure 3. Source regions used in the low-resolution, analytical inversion. The rest of the world includes emissions from outside of the five continental regions considered. It also includes the source of CO from the oxidation of CH_4 and biogenic NMVOCs.

state vector, with its associated error covariance is [*Rodgers*, 2000]

$$\hat{\mathbf{x}} = \mathbf{x_a} + \mathbf{S_a}\nabla_{\mathbf{x}}\mathbf{F}^{\mathbf{T}}\left(\nabla_{\mathbf{x}}\mathbf{F}\mathbf{S_a}\nabla_{\mathbf{x}}\mathbf{F}^{\mathbf{T}} + \mathbf{S}_{\Sigma}\right)^{-1}(\mathbf{y} - \mathbf{F}(\mathbf{x_a})) \quad (6)$$

$$\hat{\mathbf{S}}^{-1} = \nabla_{\mathbf{x}}\mathbf{F}^{\mathbf{T}}\mathbf{S}_{\Sigma}^{-1}\nabla_{\mathbf{x}}\mathbf{F} + \mathbf{S_a^{-1}}. \quad (7)$$

Computation of $\hat{\mathbf{x}}$ and $\hat{\mathbf{S}}$ requires explicit construction of the Jacobian matrix, which is done using a tagged simulation with separate atmospheric tracers for emissions from each region in the state vector, as described by *Heald et al.* [2004] and *Jones et al.* [2009]. In the low-resolution inversion the state vector consists of the five continental regions shown in Figure 3 as well as the rest of the world (ROW) and a global background chemical source.

[17] The computational cost of running separate tracers for each element of the state vector and of storing the matrices in equations (6) and (7) limit the size of the state vector. An alternative to using the analytical solution in equation (6) is to numerically minimize the cost function using a variational approach. We use the adjoint of the GEOS-Chem model [*Henze et al.*, 2007; *Kopacz et al.*, 2009] to minimize the cost function, in a four-dimensional variational (4D-VAR) approach, as described by *Kopacz et al.* [2009]. The adjoint provides a computationally efficient means of calculating the sensitivity of the CO distribution in the model to emissions from each grid box. The objective of the 4D-VAR method is to produce a model trajectory that 'best' fits the observations, which are distributed in time. The minimization of J(x) is performed using the L-BFGS-B algorithm [*Byrd et al.*, 1995].

[18] Because of the long lifetime of CO, model errors can accumulate and bias the initial CO distribution, which would, in turn, bias the top-down estimates. We therefore, correct this initial bias by scaling the modeled CO columns to match the MOPITT data on 1 June and 1 September 2000. Since MOPITT achieves global coverage only every 3 days, in a given day there are large data gaps between

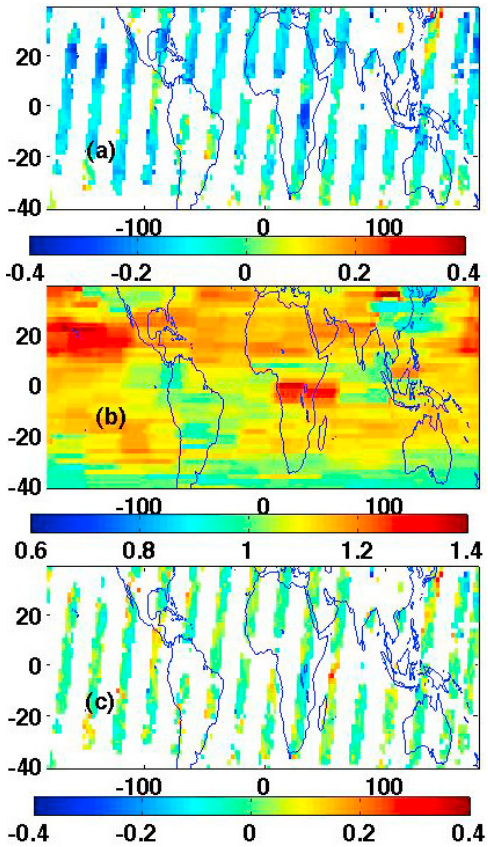

Figure 4. Correction of the initial bias in the CO distribution in the inversion. (a) Initial condition bias on 1 June 2000 for the GEOS-3 simulation. The bias is calculated as (model – MOPITT)/MOPITT. The blank grids correspond to MOPITT data gap. (b) Correction factors on 1 June 2000. (c) Bias on 1 June 2000 after scaling the CO distribution using the correction factors.

Table 1. Inversion Analysis Scaling Factors[a]

		Regions					
	Inversion Type	South America	North Africa	South Africa	Asia	Indonesia and Australia	ROW
June	a priori (Tg/month)	15.0	13.2	16.1	28.1	7.5	69.3
	analytical (COMBUS+NMVOC)	0.72	1.08	0.95	0.85	1.38	1.08
	adjoint (COMBUS+ NMVOC)	0.74	1.01	0.83	0.88	1.04	1.18
	a priori (Tg/month)	5.5	4.8	12.5	22.9	4.0	100.8
	analytical (CH_4+NMVOC)	−0.03	1.67	0.60	0.79	1.65	1.06
	adjoint (CH_4+NMVOC)	0.46	1.06	0.67	0.88	1.13	1.12
September	a priori (Tg/month)	35.1	15.5	28.0	27.7	18.8	74.6
	analytical (COMBUS+NMVOC)	0.84	0.65	0.98	0.87	1.44	1.09
	adjoint (COMBUS+NMVOC)	0.71	0.78	0.79	0.75	1.27	1.26
	a priori (Tg/month)	23.9	5.6	25.0	21.8	13.6	110.8
	analytical (CH_4+NMVOC)	0.76	0.36	0.87	0.83	1.51	1.08
	adjoint (CH_4+NMVOC)	0.55	0.61	0.75	0.67	1.43	1.17

[a]Defined as the ratio of the a posteriori to a priori emissions. The emissions for the adjoint inversion were aggregated according to the regional definitions shown in Figure 3. The rest of world (ROW) includes emissions from outside the regions in Figure 3, as well as the chemical source of CO. For the CH_4+NMVOC inversion the ROW captures the CO source from the oxidation of CH_4 and biogenic NMVOCs, whereas for the COMBUS +NMVOC inversion it includes only the source from CH_4 oxidation.

successive orbits, as shown in Figure 4a. We therefore calculate scaling factors (Figure 4b) in 50° bin in longitude for each 2° box in latitude. For the 1 June case shown in Figure 4, the global (40°S–40°N) mean bias is reduced from −10.1% to 0.07%. For 1 September (not shown) the mean bias is reduced from −5.5% to 0.1%.

[19] In their inversion analysis of the MOPITT data, *Heald et al.* [2004] and *Arellano et al.* [2004] used the observations minus model (with the a priori emissions) residuals to calculate the observation error covariance $\mathbf{S}_\Sigma$ in equation (4), which includes the measurement error and model error (transport and representativeness errors). *Arellano et al.* [2004] showed that the observation error varies between 8 and 30% of the total CO column, with model error providing the main contribution. Although the observation error is larger over the continental source regions, *Heald et al.* [2004] showed that assuming a uniform error of 20%, for example, does not significantly influence the top-down estimates for the source regions that are well constrained in the inversion. We, therefore, assume here a uniform observation error of 20%. We also neglect horizontal correlations in the observation error. We specify the a priori error covariance matrix $\mathbf{S_a}$ following *Heald et al.* [2004]. The a priori errors for the fuel combustion CO sources are based on the uncertainties reported by *Streets et al.* [2003] for Asia and are assumed to be 30% for North America and Europe, and 50% for the rest of world. Errors on the biomass burning sources are assumed to be 50% [*Palmer et al.*, 2003, 2006b; *Heald et al.*, 2004; *Kopacz et al.*, 2009, 2010], and these two errors are added in quadrature and capped at 100% to obtain the regional a priori source error. We assume that the a priori error covariance matrix is diagonal.

4. Inversion Results and Error Analysis

4.1. The Influence of Biogenic NMVOCs on the a Posteriori Estimate of Combustion Emissions

[20] Most CO inversion analyses have focused on quantifying the combustion-related emissions of CO. In these analyses [e.g., *Pétron et al.*, 2002; *Palmer et al.*, 2003; *Heald et al.*, 2004; *Arellano and Hess*, 2006; *Jones et al.*, 2009; *Kopacz et al.*, 2009, 2010] the source of CO from the oxidation of biogenic NMVOCs was typically aggregated into a global background chemical source, which, in some cases, included the source from the oxidation of CH_4. These analyses solved for estimates of the regional combustion sources and for the global chemical source. We examine here the impact of solving for a global biogenic NMVOC source on the regional combustion source estimates. When the biogenic NMVOC sources are aggregated into a global background source, they do not participate locally in the inversion. Any a priori errors in the biogenic NMVOC sources are actually accounted for in the combustion emissions. This results in an overadjustment of the combustion emissions, which could be significant in regions with weak combustion emissions and strong biogenic NMVOC sources. We note that although the combustion emissions will be overadjusted, identifying this bias by examination of the residual bias in the a posteriori model simulation is difficult since (if the observation error is small) the inversion may fit the true state well. The overadjustment will be obvious if the a priori error in the biogenic NMVOC source is positive and larger than the combustion source. In this case, correcting for the overestimate in the NMVOC source could result in negative combustion emissions.

[21] Table 1 shows the inversion results using MOPITT data for June and September 2000, with the GEOS-3 version of GEOS-Chem as the forward model. For each month we report the top-down estimates obtained with the analytical and adjoint approaches. We conduct two experiments in which the biogenic NMVOCs source is treated differently. In one experiment, referred to as CH_4+NMVOC, the CO from the oxidation of biogenic NMVOCs and CH_4 are aggregated together to construct a global chemical background. In this case we solve for the regional combustion sources and the global chemical source. In the other experiment, referred to as COMBUS+NMVOC, the biogenic NMVOC source is combined with the combustion emissions and the global chemical background contains only the contribution from CH_4 oxidation. In this experiment we solve for the total combustion and biogenic NMVOC source regionally and for a global CH_4 source. The adjoint scaling factor in Table 1 is the ratio of the a posteriori emission to the a priori emission calculated by averaging the adjoint

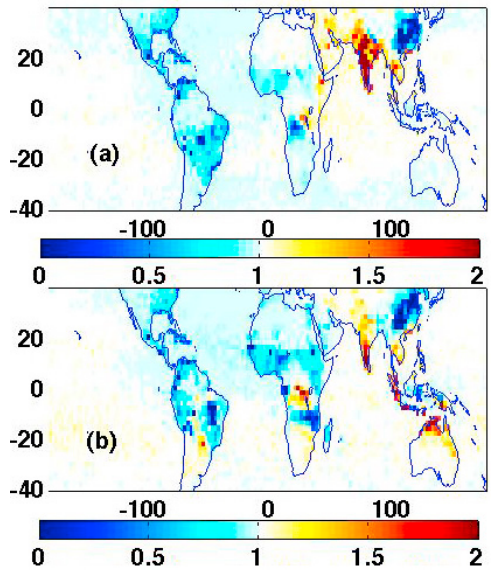

Figure 5. Scaling factors for the COMBUS+NMVOC adjoint inversion.

scaling factors according on the region definitions showed in Figure 3.

[22] Comparing the analytical and adjoint scaling factors for the CH_4+NMVOC case, we find that the largest differences between the two approaches are for the regions where the biogenic NMVOC source is comparable to or larger than the combustion-related emissions. In June, this is the case for emissions from South America, North Africa, and Indonesia/Australia. For North Africa in June, the combustion-related emissions are 4.8 Tg CO in the a priori, whereas the biogenic NMVOC source is 8.4 Tg CO in the a priori. The difference in the scaling factors, 1.67 for the analytical inversion and 1.06 for the adjoint inversion, is larger than the bias expected from aggregation error, as we will show in section 4.2. This difference, we suggest, is due to aggregating the biogenic NMVOC source into the background chemical source. If biogenic NMVOC source is instead included in the regional budget, the adjoint and analytical scaling factors are in better agreement, 1.01 and 1.08, respectively.

[23] The most significant disagreement between the adjoint and analytical scaling factors are for the South American source estimates in June (for the CH_4+NMVOC case), where analytical inversion yields a negative scaling factor of −0.03 and the adjoint inversion gives a value of 0.46. The CO source from biogenic NMVOCs is 9.5 Tg CO in June, which is much larger than the combustion source of 5.5 Tg CO. The negative scaling factor reflects an overadjustment of the emissions due to the a priori error in the biogenic NMVOC source. Combining the South American biogenic NMVOC source with the combustion emissions (the COMBUS+NMVOC case) yields a scaling factor of 0.72 for the analytical inversion in June, which is in agreement with the adjoint scaling factor of 0.74.

[24] To understand the cause of the overadjustment of the South American scaling factors, it is helpful to examine the spatial distribution of the adjoint scaling factors, shown in Figure 5a for the COMBUS+NMVOC inversion. The inversion significantly reduced the emissions in central South America (the dark blue grid boxes), where the biogenic NMVOC source is strongest (see Figure 2c). When this a priori bias in the NMOVC source is aggregated in the global background, the inversion compensates by excessively reducing the combustion-related emissions. The overcompensation is smaller in the adjoint inversion because of the greater degrees of freedom to adjust the emissions and the fact that the optimization of the emissions in these specific grid boxes stops when their scaling factor approaches zero. However, because the analytical inversion is solving for a single scaling factor for all of South America, the strong, local bias in the biogenic NMVOC source results in a significant overadjustment of the regional emissions.

[25] Another approach for quantifying the sources is to solve separately for the regional combustion and biogenic NMVOC sources, as opposed to the COMBUS+NMVOC case in which we solved for the total regional emissions. The difficulty with this approach is that if the biogenic NMVOC and combustion sources are spatially coincident, consequently the Jacobian for these sources will be similar and the inversion will be incapable of reliably distinguishing between the two source types. This behavior was noted by *Palmer et al.* [2006b] in their inversion analysis of CO_2 fluxes from fuel combustion and the biosphere. In our analytical inversion, we find that if we solve for the combustion and biogenic NMVOC sources separately, the inferred source estimates are strongly correlated. In June, for example, we obtained correlation coefficients of −0.92, −0.85, −0.68, and −0.91 for the combustion and NMVOC sources from South America, North Africa, South Africa, and Asia, respectively. In September, the combustion and NMVOC source estimates were similarly correlated. Because the CO observations provide constraints only on the total CO emitted from a given region, there is insufficient information in the inversion to reliably distinguish between the two CO fluxes when they are emitted from the same model grid box.

4.2. Aggregation Errors

[26] The adjoint scaling factors shown in Figure 5 reveal that the CO emissions from China are overestimated by the a priori source, whereas those from India are underestimated. Clearly, using a single scaling factor to uniformly adjust the emissions across Asia will introduce an aggregation error in the estimate of the Asian emissions. Associated with the error in the emissions will be a bias in the atmospheric CO abundances, for which the inversion will try to compensate and potentially introduce biases in the other elements of the state vectors. Since the 4Dvar and analytical inversion approaches are different, comparing the inferred source estimates from the two inversions does not necessarily provide a reliable estimate of the aggregation error. Furthermore, such a comparison will not enable us to assess how the aggregation error from a particular region impacts the source estimates for the other regions. As a result, we focus here on the adjoint inversion and quantify the impact of aggregation error on the state vector by conducting a series of simulation experiments in which we use the CO distribution simulated with the a posteriori source estimates from the adjoint inversion as pseudo-observations.

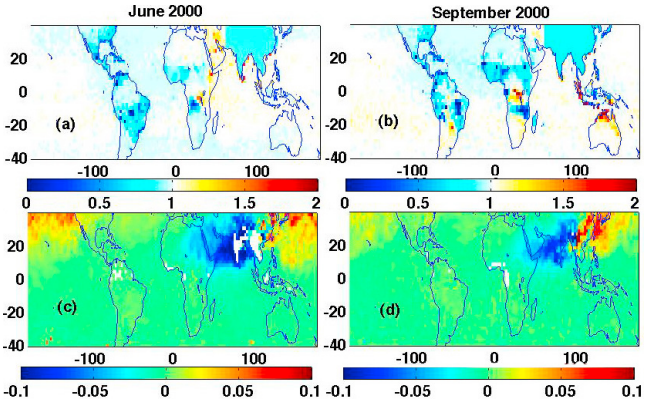

Figure 6. (a, b) Scaling factors used to scale the a priori sources for the Asian aggregation pseudoinversion experiment. (c, d) Bias in the modeled CO distribution due to the regional scaling of the Asian emissions. The bias is shown as a relative error in the upper tropospheric CO columns. The blank grids correspond to MOPITT data gap.

[27] We carry out separate inversions to assess the impact of aggregating the sources in each of the continental source regions shown in Figure 3 on all the other regions. In each case the simulated pseudodata are generated by scaling the a priori sources with the scaling factors showed in Figure 5, but with a mean scaling factor for the continental region of interest. If we use the adjoint scaling factors everywhere to generate the "true" emissions (for simulating the pseudodata) as well as the a priori emissions, the pseudoinversion will easily recover the true emissions; the scaling factors for the pseudoinversion will be unity. However, using a regional scaling factor for the Asian emissions, for example, in simulating the pseudodata, introduces an error in the simulated CO distribution, which is projected onto the state vector in the pseudoinversion and produces scaling factors that are different from unity. For Asian emissions, shown in Figures 6a and 6b, use of a mean scaling factor underestimates Indian emissions and overestimates Chinese emissions, which results in the bias in atmospheric CO shown in Figures 6c and 6d. We define the aggregation error as the impact of this bias (Figures 6c and 6d) in atmospheric CO on the sources estimates Similarly, Figure 7 showed the error caused by the aggregation of South Hemisphere Africa.

[28] Listed in Tables 2a and 2b are the results of the pseudoinversions. Each row of the table gives the aggregation error on the source estimates for the different regions created by using a regional scaling factor for a given region. If the pseudoinversions used the grid-based scaling factors everywhere, the CO distribution would be unbiased and the inversion would recover the true source estimates, with scaling factors of unity. Listed in Tables 2a and 2b are the departures of the scaling factors from unity, as a percentage, due to the regional aggregation. For example, in June, aggregating the Asian emissions in the CH_4+NMVOC inversion produces an aggregation error of 26%, 48%, and −27% in the emissions estimates for South America, North Africa, and South Africa, respectively.

[29] The dominance of the Asian aggregation error in June 2000 is due to the fact that Asia is the largest regional source of CO and because the a priori emission bias has a dipole structure (Figure 5). The inversion cannot remove the bias associated with a dipole structure by uniformly scaling the regional emissions. This explains why the aggregation error due to South Hemisphere African emissions has a small impact on the other source estimates in June, whereas it produces a 24% error in the North African estimate in September; the a priori error has a stronger dipole structure in southern tropical Africa in September (Figure 5b). This also illustrates the difficulty in conducting the inversion at a resolution that is lower than the forward model. Within the small 15° × 15° region of 0°–15°S and 10°–25°E, the a priori bias in the Africa sources is negative in June, whereas it is negative and positive in September. Without prior knowledge of the spatial and temporal distribution of the a priori bias, conducting the inversion at a resolution lower than the forward model could introduce aggregation errors.

[30] Based on the CH_4+NMVOC inversion results in Table 2a, we see that the aggregation error is largest for the weaker source regions. Thus, in June the impact of the Asian aggregation error is only 10% on the estimate for the total Asian emissions, whereas it has a significant impact on the North African emissions. Furthermore, in September when there is more biomass burning in the southern tropics, the impact of the Asian aggregation error is smaller; the aggregation error is manifested most strongly in the weaker and more poorly constrained elements of the state vector. This conclusion is supported by the aggregation error analysis for the COMBUS+NMVOC case. As can be seen in Table 1, combining the biogenic NMVOC source with the combustion emissions significantly enhanced the a priori emissions from South America, North Africa, and South Hemisphere Africa in June. As a result, the aggregation errors for the COMBUS+NMVOC inversion are much smaller, as shown in Table 2b. For example, the Asian aggregation error in the North African estimate is reduced from 48% to 12%.

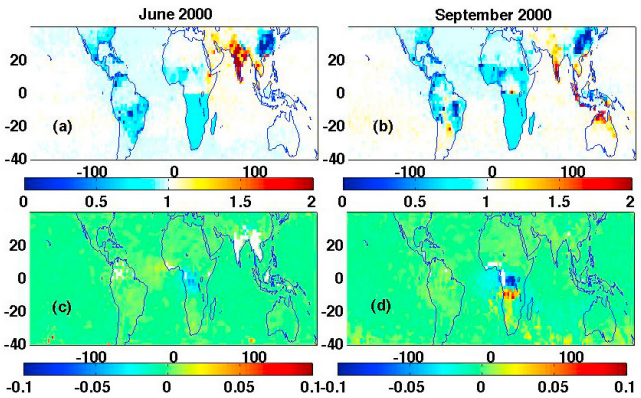

Figure 7. (a, b) Scaling factors used to scale the a priori sources for the South African aggregation pseudoinversion experiment. (c, d) Bias in the modeled CO distribution due to the regional scaling of the South African emissions. The bias is shown as a relative error in the upper tropospheric CO columns.

Table 2a. Errors in the Source Estimates Due to Regional Aggregation of the CO Sources CH_4+NMVOC[a]

CH_4+NMVOC		Aggregation Errors				
		South America	North Africa	South Africa	Asia	Indonesia and Australia
June	South America	0.4%	0.8%	−0.1%	0.5%	0.4%
	North Africa	*2.1%*	0.0%	*−1.4%*	0.7%	0.7%
	South Africa	−0.8%	0.9%	*4.4%*	0.5%	0.1%
	Asia	*−26.3%*	*48.2%*	*−26.9%*	*−9.5%*	*7.6%*
	Indonesia	−0.4%	0.3%	−0.6%	0.2%	−0.7%
September	South America	0.1%	*5.4%*	0.5%	*1.2%*	*1.1%*
	North Africa	−0.1%	*−9.1%*	*2.6%*	0.9%	0.4%
	South Africa	0.7%	*24.4%*	*−3.2%*	−0.5%	0.8%
	Asia	*−2.1%*	*26.2%*	*−4.0%*	*−5.1%*	*2.5%*
	Indonesia	−0.3%	0.8%	0.8%	0.2%	−0.3%

[a]The errors are given in percentage as departures of the pseudoinversion scaling factors from unity. Italics indicate the errors larger than 1%.

4.3. Errors in Transport and the OH Distribution

4.3.1. Impact of Errors in Transport

[31] Shown in Figure 8 is the vertical distribution of the zonal mean CO abundance in September 2000, as simulated by GEOS-Chem with the GEOS-3 and GEOS-4 meteorological fields. The strong influence of biomass burning in the southern hemisphere is evident by the maximum in CO in the southern tropical lower troposphere. The high CO abundances in the extratropical lower troposphere reflect mainly the influence of anthropogenic emissions. In the tropics, the CO mixing ratio produced with the GEOS-3 fields is significantly higher in the low troposphere. *Folkins et al.* [2006] showed that the upward convective mass fluxes in GEOS-3 are significantly weaker than in GEOS-4 and that the GEOS-3 fields lack a deep outflow layer in the upper troposphere. They found that these differences resulted in higher annual mean abundances of CO in the middle and upper troposphere in GEOS-4 than in GEOS-3, and that the CO profile in GEOS-4 decreased more rapidly with altitude near the tropopause due to the decrease in convective outflow at those altitudes in GEOS-4. Similarly, *Wu et al.* [2007] showed that GEOS-Chem with GEOS-3 has more CO in the lower troposphere than with GEOS-4, whereas the opposite occurs in the middle and upper troposphere.

[32] Table 3 compares the scaling factors for the analytical inversion for the COMBUS+NMVOC case using these two meteorological fields. The scaling factors of the GEOS-4 inversion are generally consistent with that of GEOS-3 inversion, to within about 10%, with the exception for the Indonesian/Australian region. The largest discrepancy is for Indonesia/Australia in September, when the difference between the two inversions is 22%. This is consistent with the study of *Arellano and Hess* [2006] who used three different forward models in their CO inversion and found that the largest discrepancy in the source estimates was for the Indonesian source. The other source estimates for which we found large discrepancies in September were for the Asian and South African sources, for which the errors were 9%. These errors are generally smaller than those reported by *Arellano and Hess* [2006], who found, for example, discrepancies as large as 81% for the Indonesian source. This could be due to the fact that *Arellano and Hess* [2006] used three different atmospheric CTMs driven by different meteorological fields.

4.3.2. Impact of Errors in the OH Distribution

[33] To facilitate the calculation of the Jacobian, the CO chemistry is often linearized using prescribed OH fields. In this approach changes in CO do not feedback on the OH abundances. Furthermore, although the lifetime of OH is short, transport processes do influence the distribution of OH through their impact on the distribution of the longer-lived OH precursors. Therefore, imposing the OH distribution will result in regional inconsistencies between the OH field and the meteorological fields employed in the forward model, which could introduce errors in the top-down CO source estimates. In the work by *Jones et al.* [2009] for example, the inversion was conducted using GEOS-Chem with the GEOS-4 fields as the forward model, but the OH abundances were based on a GEOS-Chem simulation using the GEOS-3 meteorology.

[34] To assess the possible impact of discrepancies in the distribution of OH on the top-down estimates, we repeated the inversions using the GEOS-4 version of GEOS-Chem, but with the OH fields obtained from the GEOS-3 simula-

Table 2b. Errors in the Source Estimates Due to Regional Aggregation of the CO Sources COMBUS+NMVOC[a]

COMBUS+NMVOC		Aggregation Errors				
		South America	North Africa	South Africa	Asia	Indonesia and Australia
June	South America	0.3%	−0.3%	*1.7%*	0.4%	−0.1%
	North Africa	0.9%	*−1.7%*	0.5%	0.8%	0.5%
	South Africa	−0.5%	−0.8%	*4.1%*	0.4%	−0.3%
	Asia	*−4.5%*	*11.9%*	*−12.0%*	*−8.3%*	*4.8%*
	Indonesia	0.7%	0.0%	0.1%	0.3%	−0.4%
September	South America	−0.6%	−0.2%	*1.7%*	0.4%	0.8%
	North Africa	−0.3%	*−4.1%*	*4.0%*	0.5%	0.4%
	South Africa	0.4%	*5.5%*	*−1.8%*	0.0%	*1.2%*
	Asia	−0.8%	*4.4%*	*−1.6%*	*−3.3%*	*3.3%*
	Indonesia	−0.2%	0.1%	0.8%	0.1%	0.8%

[a]The errors are given in percentage as departures of the pseudoinversion scaling factors from unity. Italics indicate the errors larger than 1%.

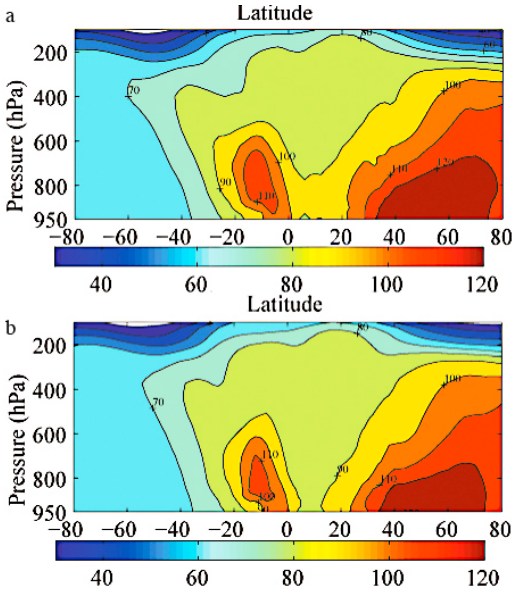

Figure 8. Zonal mean CO distribution in September 2000 as simulated by GEOS-Chem with (a) GEOS-3 meteorology and (b) GEOS-4 meteorology. Units are ppb.

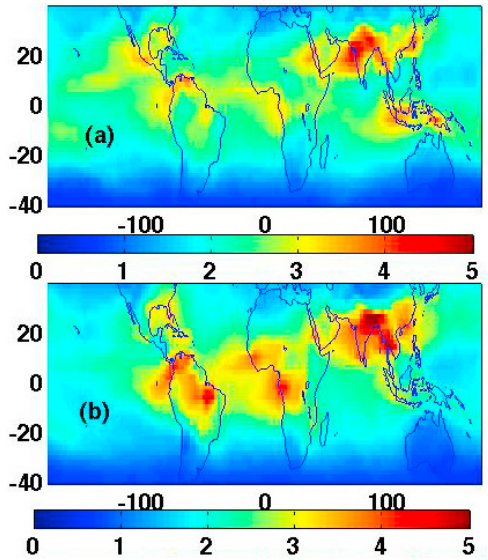

Figure 9. The mean tropospheric OH column abundance in September 2000 as simulated by GEOS-Chem with (a) GEOS-3 meteorology and (b) GEOS-4 meteorology. Units are 10^{12} molec/cm^2.

tion. The GEOS-3 OH fields are based on the simulation of *Evans and Jacob* [2005]. The OH distributions of the GEOS-4 and GEOS-3 simulations are shown in Figure 9. There is significantly more OH over South America, tropical Africa, and South Asia in GEOS-4 than that in GEOS-3. The global mean tropospheric OH concentration in GEOS-3 is 1.05×10^6 molec/cm^3, whereas in GEOS-4 it is 1.10×10^6 molec/cm^3. The regional differences in the OH distributions reflect the differences in vertical transport, as discussed above, as well as differences in cloud cover in the two meteorological fields. As shown by *Wu et al.* [2007], the photolysis rate for the production of O(^{1}D) from ozone, which is required to produce OH, is significantly greater in GEOS-4 than in GEOS-3 in the middle and upper troposphere due to differences in the cloud optical depths in the models.

[35] Figure 10 shows the bias in upper tropospheric CO between the GEOS-3 simulation and the GEOS-4 simulation with two OH fields. As can be seen in Figure 10d, the CO concentrations in GEOS-4 in the upper troposphere over southeast Asia and South America are significantly greater with the GEOS-3 OH fields. The top-down estimates from the inversions are listed in Table 3. In June the GEOS-4 inversion produces a scaling factor of 0.8 for South America, which is comparable to the scaling factor of 0.72 obtained with GEOS-3. However, using the GEOS-3 OH fields in the GEOS-4 inversion results in a scaling factor of 0.94. Similarly, for South Africa the GEOS-4 inversion suggested a scaling factor of 1.0, which is comparable to the scaling factor of 0.95 from the GEOS-3 inversion, whereas using the GEOS-3 OH in the GEOS-4 inversion produced a scaling factor of 0.79. In general, the differences in the source estimates due to the two OH fields are comparable to or larger than those obtained using the two different transport fields.

5. Conclusions

[36] We have conducted an inversion analysis of atmospheric CO to quantify the potential impact of systematic model errors on top-down CO source estimates. Using the GEOS-Chem model, our analysis examined the impact on the top-down estimates of the treatment of the biogenic NMVOC source of CO, aggregation errors, transport errors, and errors in the distribution of OH. We conducted a low-

Table 3. Scaling Factors of the COMBUS+NMVOC Low-Resolution, Analytical Inversion[a]

		Regions					
	Analytical Inversion COMBUS+NMVOC	South America	North Africa	South Africa	Asia	Indonesia and Australia	ROW
June	a priori (Tg/month)	15.0	13.2	16.1	28.1	7.5	69.3
	GEOS-3	0.72	1.08	0.95	0.85	1.38	1.08
	GEOS-4 with G-3 OH	0.94	1.15	0.79	0.82	1.39	1.04
	GEOS-4	0.80	1.11	1.00	0.83	1.19	1.12
September	a priori (Tg/month)	35.1	15.5	28.0	27.7	18.8	74.6
	GEOS-3	0.84	0.65	0.98	0.87	1.44	1.09
	GEOS-4 with G-3 OH	0.85	0.50	0.99	0.85	1.33	1.13
	GEOS-4	0.89	0.69	1.07	0.96	1.22	1.08

[a]The GEOS-3 and GEOS-4 results were obtained using GEOS-Chem with the GEOS-3 and GEOS-4 meteorology, respectively, and with consistent OH fields. The GEOS-4 with G-3 OH results were obtained by running GESO-Chem with GEOS-4 meteorology and with OH fields from the GEOS-3 simulation.

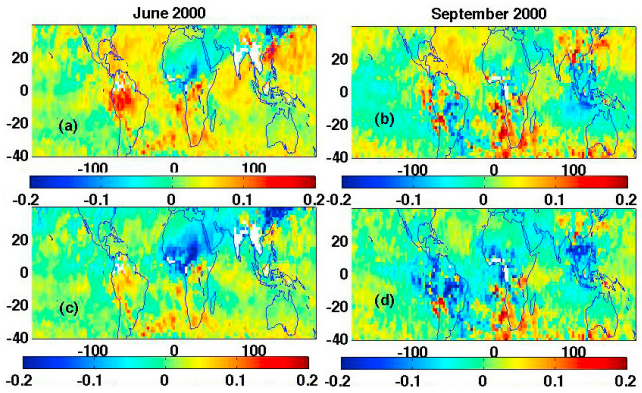

Figure 10. Model bias between GEOS-3 and GEOS-4, calculated as (GEOS-3 – GEOS-4)/GEOS-3. The bias reflects the relative error in the upper tropospheric CO columns (for altitudes above the 500 hPa pressure level). (a, b) The GEOS-4 simulation uses GEOS-4 OH fields, whereas (c, d) the GEOS-4 simulation uses GEOS-3 OH fields.

resolution analytical inversion, based on the work by *Heald et al.* [2004], and a high-resolution, adjoint inversion, following *Kopacz et al.* [2009]. We focused on CO sources in the tropics, where biogenic emissions and biomass burning provide strong, distinct sources of CO. To assess how the impact of the model errors is influenced by the strength of the sources, we used MOPITT satellite observations of CO in June 2000, before the biomass burning season in South America and when biomass burning in South Africa is weak, and in September 2000, when biomass burning emissions from South America and South Africa are strong.

[37] Most previous inversion analyses of CO have focused on quantifying the combustion-related emissions of CO and aggregated the biogenic NMVOC source into a global background chemical source. We found that aggregating the a priori bias in the biogenic NMVOC source into a global background can significantly bias the source estimates, as it limits the ability of the inversion to compensate for the regional a priori biogenic NMVOC bias, which results in an overadjustment of the estimate of the regional emissions. The error can be large if the regional biogenic NMVOC source is comparable to or larger than the combustion emissions. In the lower-resolution inversion, this overadjustment can result in negative regional emissions.

[38] Solving for the combined combustion and biogenic source reduced the overadjustment of the top-down estimates. This reflects the fact that observations of atmospheric CO alone do not provide enough degrees of freedom to disaggregate colocated sources of CO. However, there is a policy-relevant need to better quantify the combustion emissions, independent of the biogenic sources. One way of doing this would be to include observations of formaldehyde (HCHO) in the inversion as a constraint on the biogenic sources. Space-based observations of HCHO have previously been used to infer top-down estimates of isoprene emissions [e.g., *Palmer et al.*, 2003, 2006a; *Shim et al.*, 2005; *Millet et al.*, 2008; *Stavrakou et al.*, 2009]. A two-step approach in which the HCHO data are first used to estimate the biogenic emissions, which are then used in the CO inversion as a strong a priori constraint would help to better quantify the combustion-related emissions. Alternatively, the HCHO and CO data could be used in a joint CO-HCHO inversion to quantify the combustion and biogenic NMVOC sources of CO.

[39] We found that aggregation error, caused by solving for the emissions on spatial scales larger then the forward model, had a significant influence on the top-down source estimates. The source estimates for the strong emission regions were generally insensitive to the aggregation errors, but the bias in the source estimates for the weaker emission regions was large; the error was 48% for the North African source estimate in June. We found that the aggregated regions in which the a priori emission bias changed sign contributed the most to the aggregation errors since the inversion cannot correct such a bias with a uniform scaling factor. Since the structure of the a priori bias is usually unknown before the inversion is conducted, our results suggest that the inversion analysis should be conducted at the resolution of the forward model to obtain the most reliable estimates of the sources.

[40] Using the differences in the CO distribution obtained with the GEOS-3 and GEOS-4 meteorological fields as a potential measure of transport error, we found that the differences in the transport fields could introduce an error of as much as 20% on the source estimates. The largest error was obtained for the emissions estimate for the Australian/Indonesian region, where convective transport plays an important role in the export of the CO emissions. This was consistent with the findings of *Arellano and Hess* [2006], who obtained differences that were as large as 40% for the emission estimates for Indonesia, South America, Europe, and Asia based on the three forward models considered in their inversion analysis.

[41] We also examined the impact of discrepancies in atmospheric OH in the source estimates. Using the GEOS-4 version of GEOS-Chem with specified OH fields based on the GEOS-3 and GEOS-4 simulations, we estimated differences in the source estimates of as much 20%, which were comparable to the differences in the estimates obtained using the two different transport fields. These differences in the top-down estimates are much larger than the a posteriori uncertainties of the source estimates typically obtained in the inversion analyses. For example, in their inversion analysis of MOPITT data, *Jones et al.* [2009] estimated a posteriori uncertainties of a few percent for their top-down estimates of the regional emissions considered here. Our results suggest that systematic errors in the atmospheric models are a significant limitation for the accuracy of the top-down source estimates of CO.

[42] It is important to consider that our conclusions are not limited only to CO inversions. Aggregation and model transport errors will have significant impacts on the inversion analyses of other atmospheric tracers, such as CO_2. Furthermore, in the case of CO_2, solving for the biospheric fluxes, while neglecting the combustion-related sources, as is traditionally done [e.g., *Gurney et al.*, 2002; *Baker et al.*, 2006], could bias the CO_2 flux estimates where there are large local biases in the combustion source. The work presented here suggests that obtaining reliable top-down emission inventories will require a more comprehensive assessment of the impact of model biases on atmospheric inversion analyses.

[43] **Acknowledgments.** This work was supported by funding from the Natural Sciences and Engineering Research Council of Canada (NSERC). The GEOS-Chem model is managed by the Atmospheric Chemistry Modeling Group at Harvard University with support from the NASA Atmospheric Chemistry Modeling and Analysis Program (ACMAP).

References

Allen, D., K. Pickering, and M. Fox-Rabinovitz (2004), Evaluation of pollutant outflow and CO sources during TRACE-P using model-calculated, aircraft-based, and Measurements of Pollution in the Troposphere (MOPITT)–derived CO concentrations, *J. Geophys. Res.*, *109*, D15S03, doi:10.1029/2003JD004250.

Arakawa, A., and W. H. Schubert (1974), Interaction of a cumulus cloud ensemble with the large-scale environment, Part I, *J. Atmos. Sci.*, *31*, 674–701, doi:10.1175/1520-0469(1974)031<0674:IOACCE>2.0.CO;2.

Arellano, A. F., Jr., and P. G. Hess (2006), Sensitivity of top-down estimates of CO sources to GCTM transport, *Geophys. Res. Lett.*, *33*, L21807, doi:10.1029/2006GL027371.

Arellano, A. F., Jr., P. S. Kasibhatla, L. Giglio, G. R. van der Werf, and J. T. Randerson (2004), Top-down estimates of global CO sources using MOPITT measurements, *Geophys. Res. Lett.*, *31*, L01104, doi:10.1029/2003GL018609.

Baker, D. F., et al. (2006), Transcom 3 inversion intercomparison: Impact of transport model errors on the interannual variability of regional CO_2 fluxes, 1988–2003, *Global Biogeochem. Cycles*, *20*, GB1002, doi:10.1029/2004GB002439.

Bey, I., et al. (2001), Global modeling of tropospheric chemistry with assimilated meteorology: Model description and evolution, *J. Geophys. Res.*, *106*, 23,073–23,095, doi:10.1029/2001JD000807.

Byrd, R. H., P. Lu, J. Nocedal, and C. Zhu (1995), A limited memory algorithm for bound constrained optimization, *SIAM J. Sci. Comput.*, *16*(5), 1190–1208, doi:10.1137/0916069.

Carmichael, G. R., et al. (2003), Evaluating regional emission estimates using the TRACE-P observations, *J. Geophys. Res.*, *108*(D21), 8810, doi:10.1029/2002JD003116.

Deeter, M. N., et al. (2003), Operational carbon monoxide retrieval algorithm and selected results for the MOPITT instrument, *J. Geophys. Res.*, *108*(D14), 4399, doi:10.1029/2002JD003186.

Deeter, M. N., D. P. Edwards, J. C. Gille, and J. R. Drummond (2007a), Sensitivity of MOPITT observations to carbon monoxide in the lower troposphere, *J. Geophys. Res.*, *112*, D24306, doi:10.1029/2007JD008929.

Deeter, M. N., D. P. Edwards, and J. C. Gille (2007b), Retrievals of carbon monoxide profiles from MOPITT observations using lognormal a priori statistics, *J. Geophys. Res.*, *112*, D11311, doi:10.1029/2006JD007999.

Duncan, B. N., R. V. Martin, A. C. Staudt, R. Yevich, and J. A. Logan (2003), Interannual and seasonal variability of biomass burning emissions constrained by satellite observations, *J. Geophys. Res.*, *108*(D2), 4100, doi:10.1029/2002JD002378.

Duncan, B. N., et al. (2007), Global budget of CO, 1988–1997: Source estimates and validation with a global model, *J. Geophys. Res.*, *112*, D22301, doi:10.1029/2007JD008459.

Emmons, L. K., et al. (2004), Validation of Measurements of Pollution in the Troposphere (MOPITT) CO retrievals with aircraft in situ profiles, *J. Geophys. Res.*, *109*, D03309, doi:10.1029/2003JD004101.

Evans, M. J., and D. J. Jacob (2005), Impact of new laboratory studies of N_2O_5 hydrolysis on global model budgets of tropospheric nitrogen oxides, ozone, and OH, *Geophys. Res. Lett.*, *32*, L09813, doi:10.1029/2005GL022469.

Folkins, I., et al. (2006), Testing convective parameterizations with tropical measurements of HNO_3, CO, H_2O, and O_3: Implications for the water vapor budget, *J. Geophys. Res.*, *111*, D23304, doi:10.1029/2006JD007325.

Gurney, K. R., et al. (2002), Towards robust regional estimates of CO_2 sources and sinks using atmospheric transport models, *Nature*, *415*, 626–630, doi:10.1038/415626a.

Hack, J. J. (1994), Parameterization of moist convection in the National Center for Atmospheric Research community climate model (CCM2), *J. Geophys. Res.*, *99*(D3), 5551–5568, doi:10.1029/93JD03478.

Heald, C. L., et al. (2004), Comparative inverse analysis of satellite (MOPITT) and aircraft (TRACE-P) observations to estimate Asian sources of carbon monoxide, *J. Geophys. Res.*, *109*, D23306, doi:10.1029/2004JD005185.

Henze, D. K., A. Hakami, and J. H. Seinfeld (2007), Development of the adjoint of GEOS-Chem, *Atmos. Chem. Phys.*, *7*, 2413–2433, doi:10.5194/acp-7-2413-2007.

Jones, D. B. A., K. W. Bowman, J. A. Logan, C. L. Heald, J. Liu, M. Luo, J. Worden, and J. Drummond (2009), The zonal structure of tropical O_3 and CO as observed by the Tropospheric Emission Spectrometer in November 2004–Part 1: Inverse modeling of CO emissions, *Atmos. Chem. Phys.*, *9*, 3547–3562, doi:10.5194/acp-9-3547-2009.

Kaminski, T., P. J. Rayner, M. Heimann, and I. G. Enting (2001), On aggregation errors in atmospheric transport inversions, *J. Geophys. Res.*, *106*, 4703–4715, doi:10.1029/2000JD900581.

Kopacz, M., et al. (2009), Comparison of adjoint and analytical Bayesian inversion methods for constraining Asian sources of carbon monoxide using satellite (MOPITT) measurements of CO columns, *J. Geophys. Res.*, *114*, D04305, doi:10.1029/2007JD009264.

Kopacz, M., et al. (2010), Global estimates of CO sources with high resolution by adjoint inversion of multiple satellite datasets (MOPITT, AIRS, SCIAMACHY, TES), *Atmos. Chem. Phys.*, *10*, 855–876, doi:10.5194/acp-10-855-2010.

Millet, D. B., D. J. Jacob, K. F. Boersma, T. M. Fu, T. P. Kurosu, K. Chance, C. L. Heald, and A. Guenther (2008), Spatial distribution of isoprene emissions from North America derived from formaldehyde column measurements by the OMI satellite sensor, *J. Geophys. Res.*, *113*, D02307, doi:10.1029/2007JD008950.

Palmer, P. I., D. J. Jacob, A. M. Fiore, R. V. Martin, K. Chance, and T. P. Kurosu (2003), Mapping isoprene emissions over North America using formaldehyde column observations from space, *J. Geophys. Res.*, *108*(D6), 4180, doi:10.1029/2002JD002153.

Palmer, P. I., et al. (2006a), Quantifying the seasonal and interannual variability of North American isoprene emissions using satellite observations of the formaldehyde column, *J. Geophys. Res.*, *111*, D12315, doi:10.1029/2005JD006689.

Palmer, P. I., et al. (2006b), Using CO_2:CO correlations to improve inverse analyses of carbon fluxes, *J. Geophys. Res.*, *111*, D12318, doi:10.1029/2005JD006697.

Pétron, G., et al. (2002), Inverse modeling of carbon monoxide surface emissions using CMDL network observations, *J. Geophys. Res.*, *107*(D24), 4761, doi:10.1029/2001JD001305.

Rodgers, C. D. (2000), *Inverse Methods for Atmospheric Sounding: Theory and Practice*, World Sci., Singapore.

Shim, C., Y. Wang, Y. Choi, P. I. Palmer, D. S. Abbot, and K. Chance (2005), Constraining global isoprene emissions with Global Ozone Monitoring Experiment (GOME) formaldehyde column measurements, *J. Geophys. Res.*, *110*, D24301, doi:10.1029/2004JD005629.

Stavrakou, T., and J. F. Müller (2006), Grid-based versus big region approach for inverting CO emissions using Measurement of Pollution in the Troposphere (MOPITT) data, *J. Geophys. Res.*, *111*, D15304, doi:10.1029/2005JD006896.

Stavrakou, T., et al. (2009), Global emissions of non-methane hydrocarbons deduced from SCIAMACHY formaldehyde columns through 2003–2006, *Atmos. Chem. Phys.*, *9*, 3663–3679, doi:10.5194/acp-9-3663-2009.

Streets, D. G., et al. (2003), An inventory of gaseous and primary aerosol emissions in Asia in the year 2000, *J. Geophys. Res.*, *108*(D21), 8809, doi:10.1029/2002JD003093.

Wu, S., et al. (2007), Why are there large differences between models in global budgets of tropospheric ozone?, *J. Geophys. Res.*, *112*, D05302, doi:10.1029/2006JD007801.

Yevich, R., and J. A. Logan (2003), An assessment of biofuel use and burning of agricultural waste in the developing world, *Global Biogeochem. Cycles*, *17*(4), 1095, doi:10.1029/2002GB001952.

Zhang, G. J., and N. A. McFarlane (1995), Sensitivity of climate simulations to the parameterization of cumulus convection in the Canadian Climate Centre General Circulation Model, *Atmos. Ocean*, *33*, 407–46.

C. Heald, Department of Atmospheric Science, Colorado State University, Fort Collins, CO 80523, USA.

D. K. Henze, Department of Mechanical Engineering, University of Colorado, Boulder, CO 80309, USA.

Z. Jiang and D. B. A. Jones, Department of Physics, University of Toronto, Toronto, ON M5S 1A1, Canada. (zjiang@atmosp.physics.utoronto.ca)

M. Kopacz, Woodrow Wilson School of Public and International Affairs, Princeton University, Princeton, NJ 08544, USA.

J. Liu, Air Quality Research Division, Science and Technology Branch, Environment Canada, Downsview, ON M3H 5T4, Canada.